

solution of sodium carbonate (21.0 mmol, 2.226 g) and compound **6** (1.281 g, 4.29 mmol) under an Ar atmosphere. The resultant solution was stirred and refluxed at 110°C overnight. The reaction mixture was cooled to room temperature and filtered. The obtained solution was extracted by toluene (50 mL×3) and washed by brine solution (100 mL×1). The obtained organic layer was dried over with sodium sulfate and concentrated under vacuum. The resultant crude product was purified by column chromatography (silica gel: 250 mL, hexane: ethyl acetate = 10:1→ 3:1) and compound **7** was obtained as orange oil (1.444 g, 2.85 mmol, yields 68%).

Compound **7** (1.444 g, 2.85 mmol) was dissolved in methanol (30 mL) in a 100 mL flask. Conc. HCl (2 mL) was added and stirred for 3 hours at room temperature. After that, saturated NaHCO₃ aq. (50 mL) was added. This solution was extracted with diethyl ether (50 mL). This obtained water phase was neutralized used 1M-HCl and extracted with diethyl ether 50 mL and combined former obtained organic phase. The combined organic phase was washed with brine solution (100 mL) and dried over with Na₂SO₄ and concentrated under reduced pressure. Obtained brown powder washed with hexane (100 mL), so H₄BP was obtained as pale brown powder without further purification (0.641 g, 1.96 mmol, yields 69%). ¹H-NMR (400 MHz, CD₃OD, ppm, Figure S1) 1.41(s, 9H), 6.82(d, 1H), 6.84(d, 1H).

(Reference)

1. Y. Suenaga, Y. Umehata, Y. Hirano, T. Minematsu, C. G. Pierpont, *Inorg. Chim. Acta*, 2008, **361**, 2941-2949.

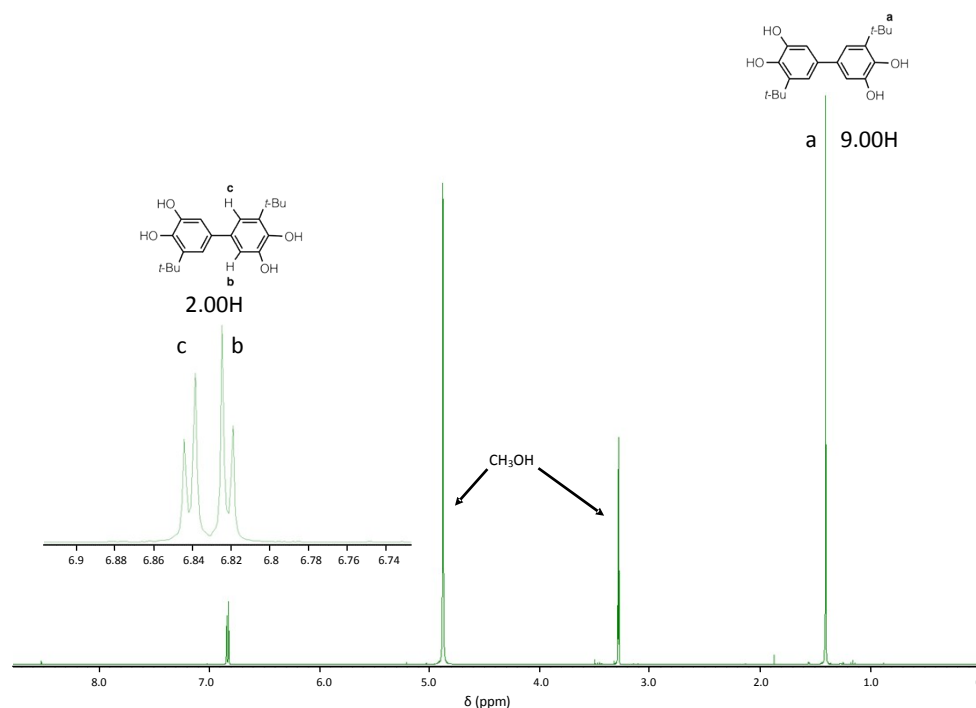


Figure S1. ¹H-NMR spectrum in CD₃OD of H₄BP

ESI-MS of $[\text{Co}_2(\text{BP})(\text{tpa})_2](\text{PF}_6)_2$ (1):

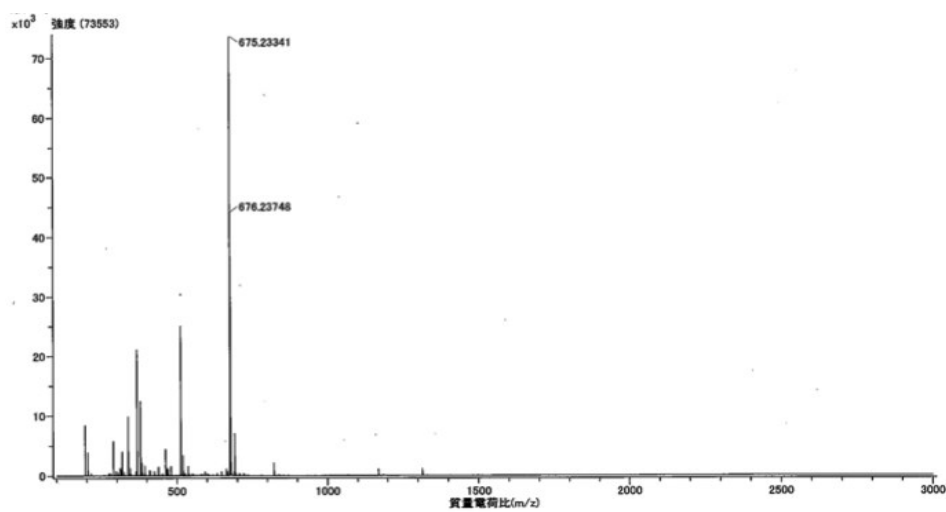


Figure S2. ESI-MS spectrum of $[\text{Co}_2(\text{BP})(\text{tpa})_2](\text{PF}_6)_2$ (1)

ESI-MS of $[\text{Co}_2(\text{BP})(\text{tpa})_2](\text{PF}_6)_3$ (2):

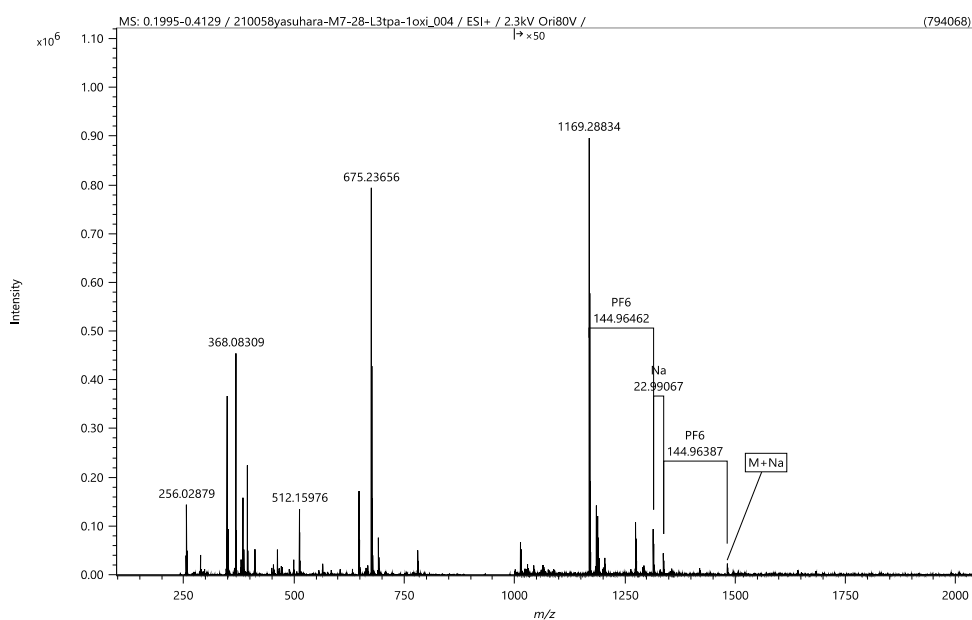


Figure S3. ESI-MS spectrum of $[\text{Co}_2(\text{BP})(\text{tpa})_2](\text{PF}_6)_3$ (2)

ESI-MS of $[\text{Co}_2(\text{BP})(\text{bpqa})_2](\text{PF}_6)_2$ (3):

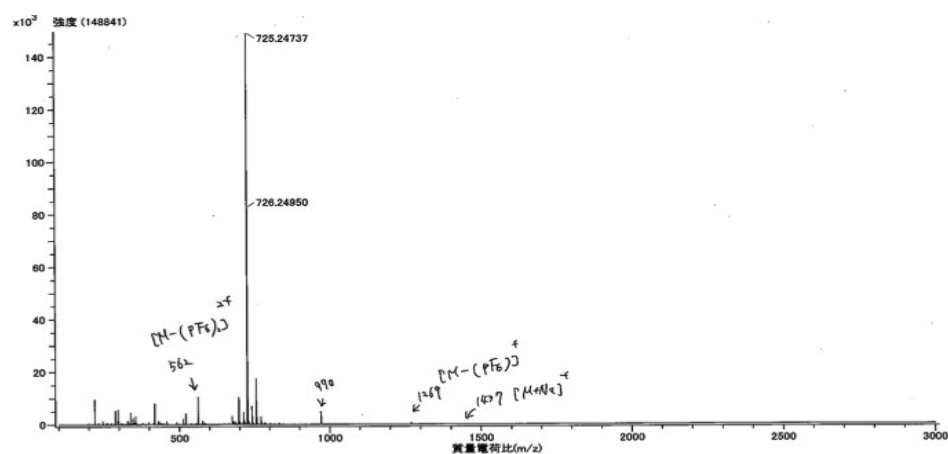


Figure S4. ESI-MS spectrum of $[\text{Co}_2(\text{BP})(\text{bpqa})_2](\text{PF}_6)_2$ (3)

ESI-MS of $[\text{Co}_2(\text{BP})(\text{pbqa})_2](\text{PF}_6)_2$ (4):

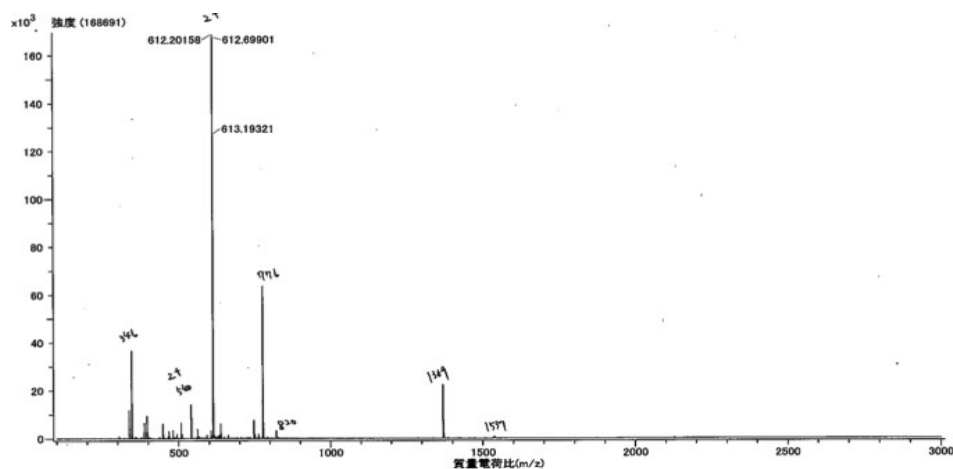


Figure S5. ESI-MS spectrum of $[\text{Co}_2(\text{BP})(\text{pbqa})_2](\text{PF}_6)_2$ (4)

ESI-MS of $[\text{Co}_2(\text{BP})(\text{tqa})_2](\text{PF}_6)_2$ (5):

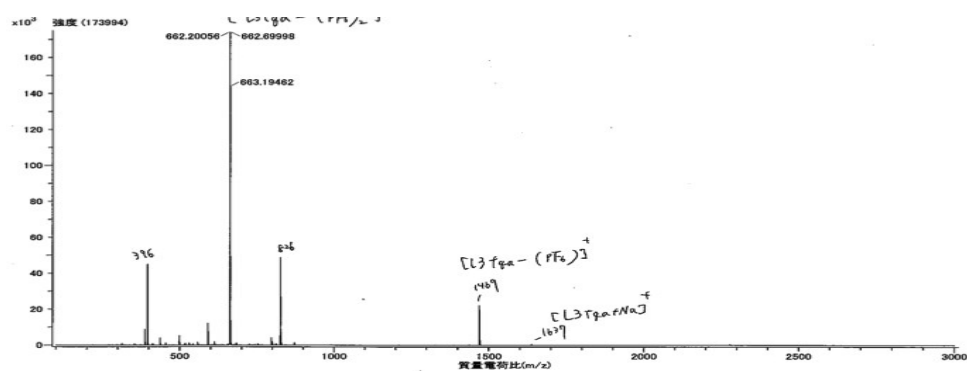


Figure S6. ESI-MS spectrum of $[\text{Co}_2(\text{BP})(\text{tqa})_2](\text{PF}_6)_2$ (5)

IR spectra

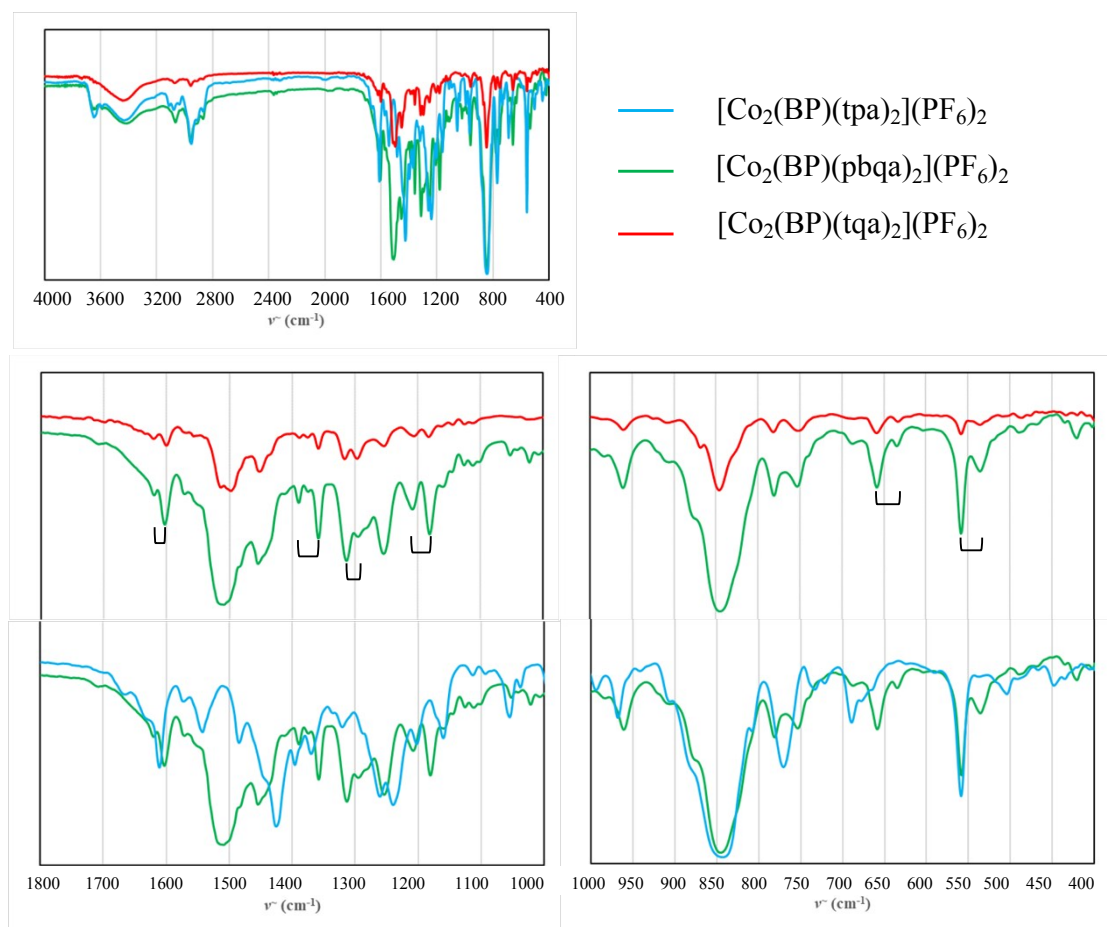


Figure S7. IR spectra of dinuclear Co complexes.

UV-Vis-NIR spectra

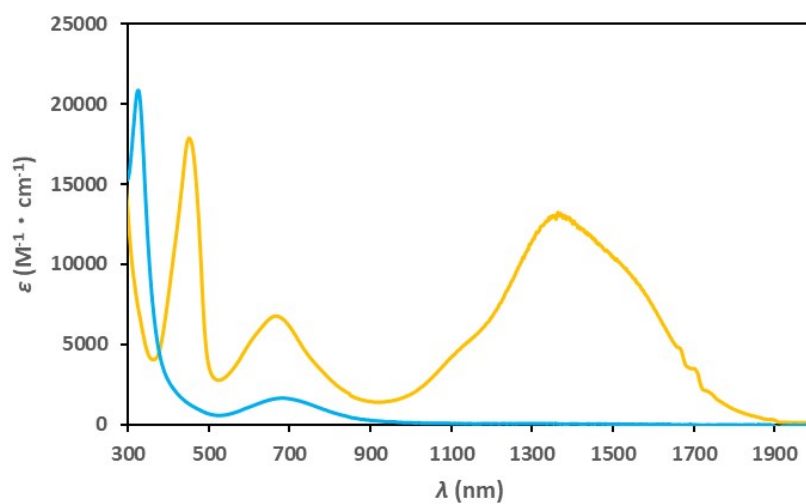


Figure S8. UV-Vis-NIR spectra of dinuclear Co complexes. blue line: $[\text{Co}_2(\text{BP})(\text{tpa})_2](\text{PF}_6)_2$ (1), yellow line: $[\text{Co}_2(\text{BP})(\text{tpa})_2](\text{PF}_6)_3$ (2) in acetonitrile solution at room temperature.

EPR spectrum for complex (2)

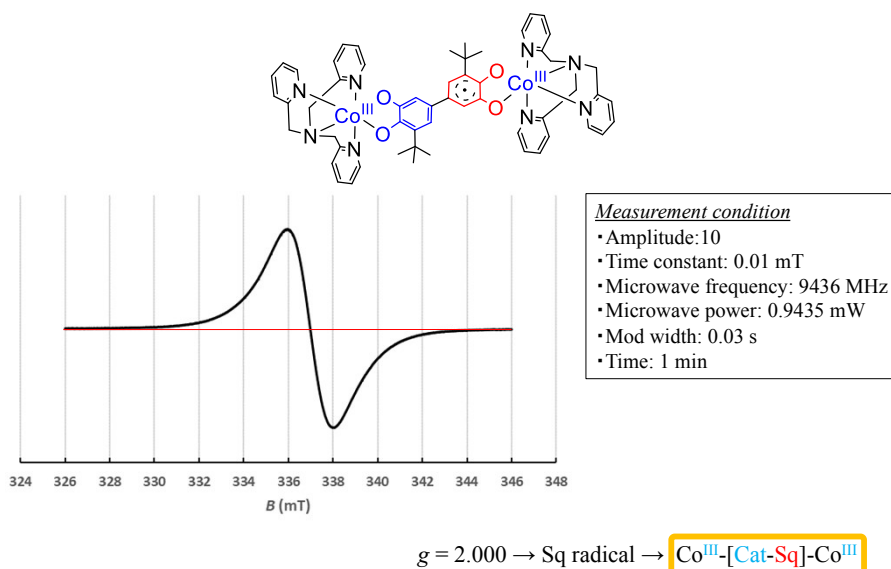


Figure S9. EPR spectrum of $[\text{Co}_2(\text{BP})(\text{tpa})_2](\text{PF}_6)_3$ (2) at room temperature.

IVCT parameters

Table S1. Mixed-valence and IVCT parameters for complex (2)

	$\Delta diox$	H_{AB1}	H_{AB2}	H_{AB3} limit	$2H_{AB1}/v_{max}$	$2H_{AB2}/v_{max}$	Γ	MV Class
	mV	cm^{-1}	cm^{-1}	cm^{-1}				
Complex (2)	377	1218	362	3645	0.33	0.10	0.47	II-III
Complex (5a) ^{*)}	175	184	1990	2820	0.07	0.71	-0.85	II-III
Pd complex ^{**)}	365	1530	3290	3710	>0.41	0.89	0.52	II-III

*) G. K. Gransbury, *et al.*, *J. Am. Chem. Soc.*, 2020, **142**, 10692-10704.

***) A. L. Poddel'sky, *et al.*, *Russ. J. Coord. Chem.*, 2012, **38**, 284-294.

Analysis of various temperature in UV-Vis-NIR spectra

The thermal variation of the fraction of $hs\text{Co}^{\text{II}}(\text{Sq})$ species determined by spectral deconvolution appears to sigmoidal profile (Figure S10).

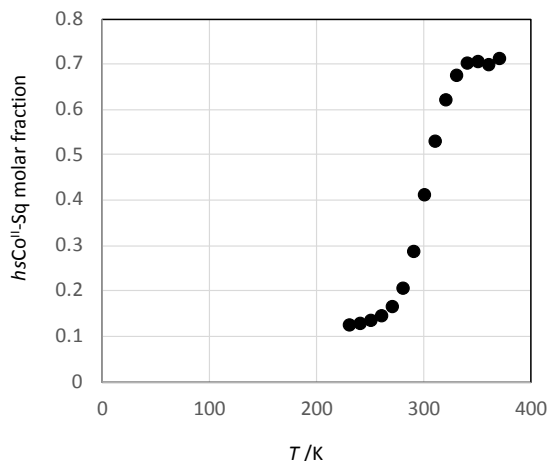


Figure S10. Temperature dependence of the molar fraction of $hs\text{Co}^{\text{II}}\text{-Sq}$ for $[\text{Co}_2(\text{BP})(\text{bpqa})_2](\text{PF}_6)_2$ (3).

Cyclic voltammetry

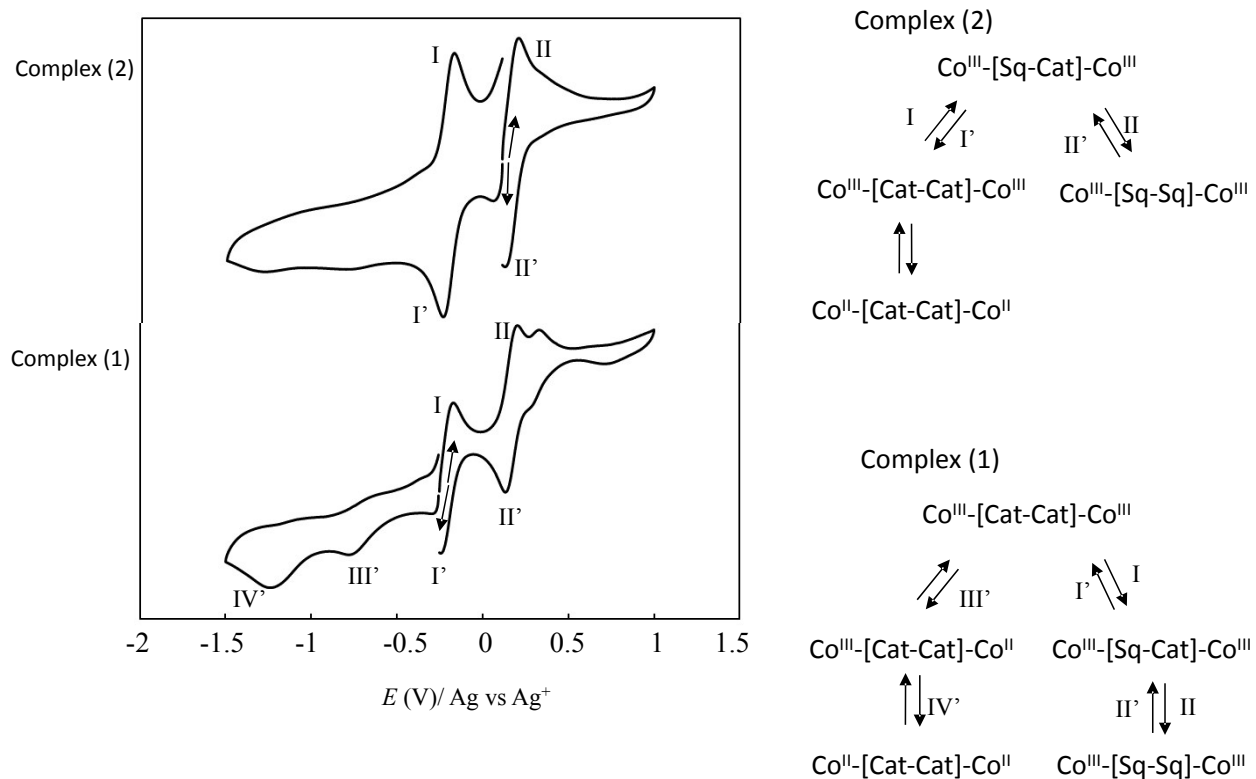


Figure S11. Cyclic voltammogram of complex(1) and (2) in acetonitrile solution at room temperature.

Table S2. Cyclic voltammetry for dinuclear Co complexes in CH_3CN

Complex	Rest potential /V	$E_{1/2} (V)/\Delta E_p(mV)$			
		I/I'	II/II'	III'	IV'
(1)	-0.25	-0.194 (73)	0.169 (54)	~-0.8	~-1.3
(2)	0.108	-0.203 (68)	0.174 (85)	-	-

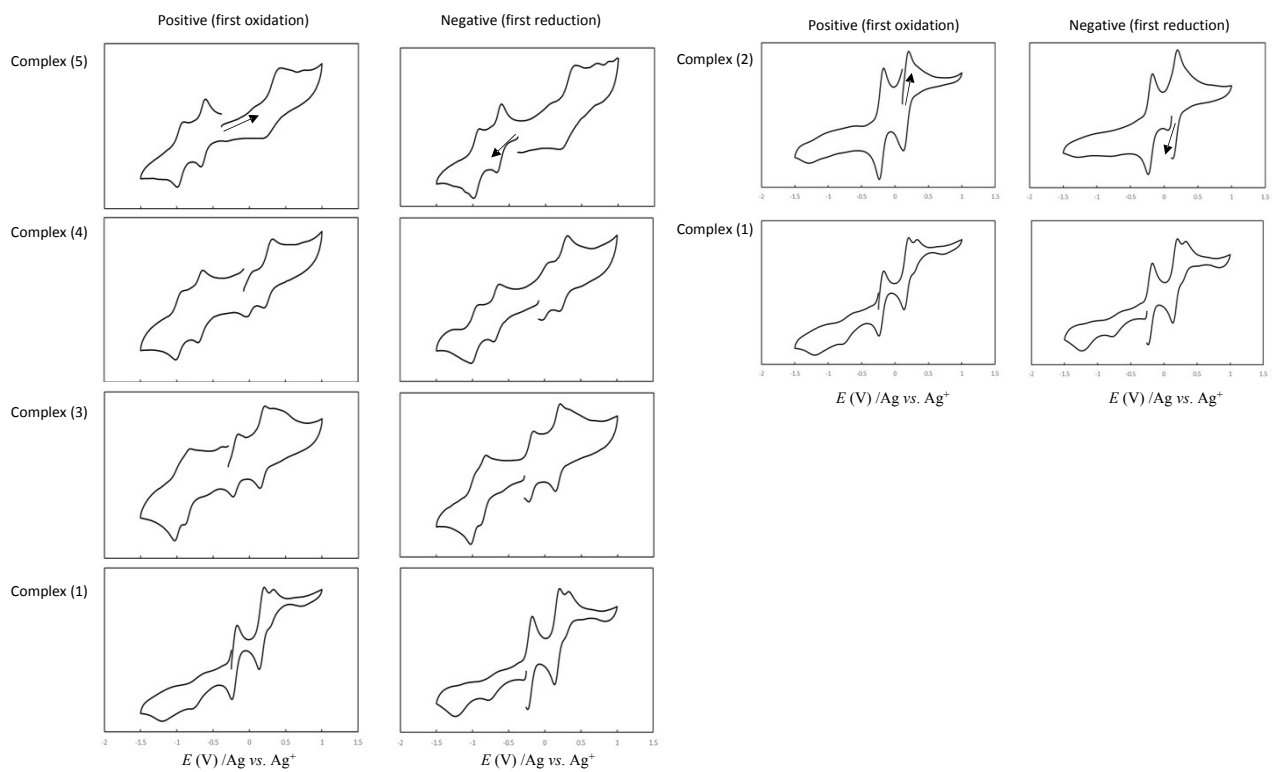


Figure S12. Cyclic voltammery of these complexes in acetonitrile at room temperature.

Crystallography

Table S3. Crystallographic data for [Co₂(BP)(tqa)₂](PF₆)₂ (5) and [Co₂(BP)(pbqa)₂](PF₆)₂ (4)

	[Co ₂ (BP)(tqa) ₂](PF ₆) ₂ (5)	[Co ₂ (BP)(pbqa) ₂](PF ₆) ₂ (4)
Chemical formula	C ₈₀ H ₇₀ Co ₂ N ₈ O ₄ F ₁₂ P ₂ · 3(C ₃ H ₆ O)	C ₇₂ H ₆₆ Co ₂ N ₈ O ₄ F ₁₂ P ₂ · 2(C ₃ H ₆ O)
Formula weight	1963.70	1863.59
Crystal system	monoclinic	monoclinic
Space group	<i>P</i> 21/ <i>m</i>	<i>P</i> 21/ <i>m</i>
Lattice Parameters		
<i>a</i> /Å	9.2480(3)	9.1110(4)
<i>b</i> /Å	41.0134(12)	41.1206(10)
<i>c</i> /Å	12.2659(5)	12.1350(3)
β /°	103.376(4)	102.590(3)
Unit Cell Volume		
<i>V</i> /Å ³	4526.2(3)	4437.1(3)
<i>Z</i>	2	2
μ (Mo-K α)/cm ⁻¹	0.71073	0.71073
No. reflections measured	10397	10309
No. observed reflections	6921	8386
[<i>I</i> > 2 σ (<i>I</i>)]		
<i>R</i> <i>I</i>	0.0636	0.1069
<i>WR</i> ₂	0.1717	0.2344
T/K	100	100
GOF	1.009	1.128
Max/Min residual electron densities	0.562/-0.529	0.709/-0.428
Measurement	Rigaku XtaLAB P200	Rigaku XtaLAB P200
Programs systems	SHELXL 2018	SHELXL 2018
Structure determination	Olex 2	Olex 2
CCDC deposition number	2067474	2067516

$$R = \frac{\sum ||F_o| - |F_c||}{\sum |F_o|}, R_w = \left[\frac{\sum \omega (F_o^2 - F_c^2)^2}{\sum \omega (F_o^2)^2} \right]^{1/2}$$

Table S4. Selected distances (Å) and angles (°) for [Co₂(BP)(pbqa)₂](PF₆)₂ (4)

Bond	Distances (Å)	Bond	Distances (Å)
Co1-O1	2.145(3)	Co1-O2	1.973(3)
Co1-N1	2.141(4)	Co1-N2	2.166(5)
Co1-N3	2.164(5)	Co1-N4	2.139(3)
C1-O2	1.300(6)	C6-O1	1.256(5)
C1-C2	1.380(6)	C2-C3	1.400(6)
C3-C4	1.436(6)	C4-C5	1.359(6)
C5-C6	1.446(6)	C6-C1	1.467(6)
Bond	Angles (°)	Bond	Angles (°)
O1-Co1-O2	79.3(1)	O2-Co1-N4	104.5 (1)
N4-Co1-N1	82.8(1)	N1-Co1-O1	93.3(1)
N2-Co1-N3	156.1(2)		

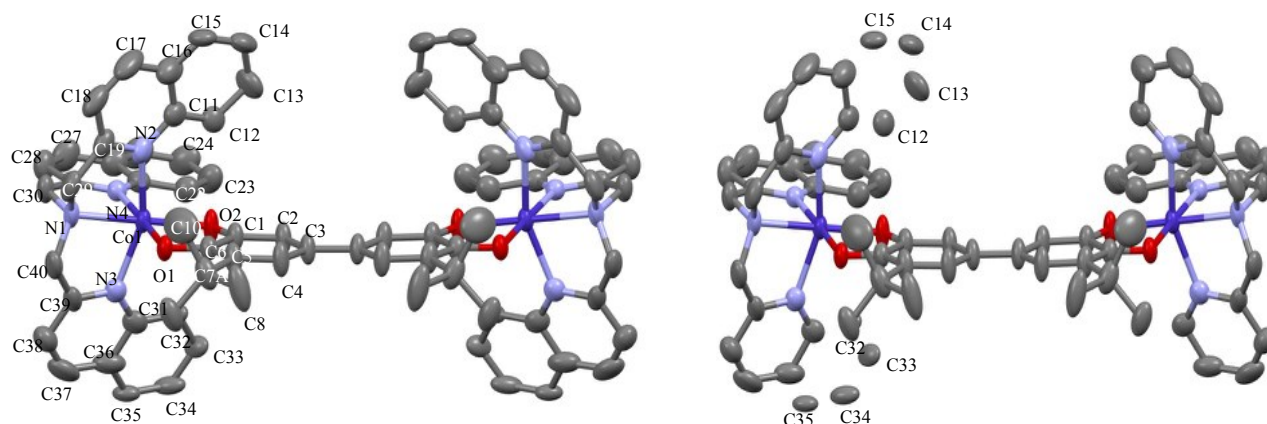


Figure S13. Perspective view of the complex cation in [Co₂(BP)(pbqa)₂](PF₆)₂ (4) showing 50% thermal ellipsoids. Hydrogen atoms and the PF₆ anions are omitted for the sake of clarity. Right: drawing the disorder axial quinoline rings (C12~C15 and C32~C35) due to structural rearrangement of complex.

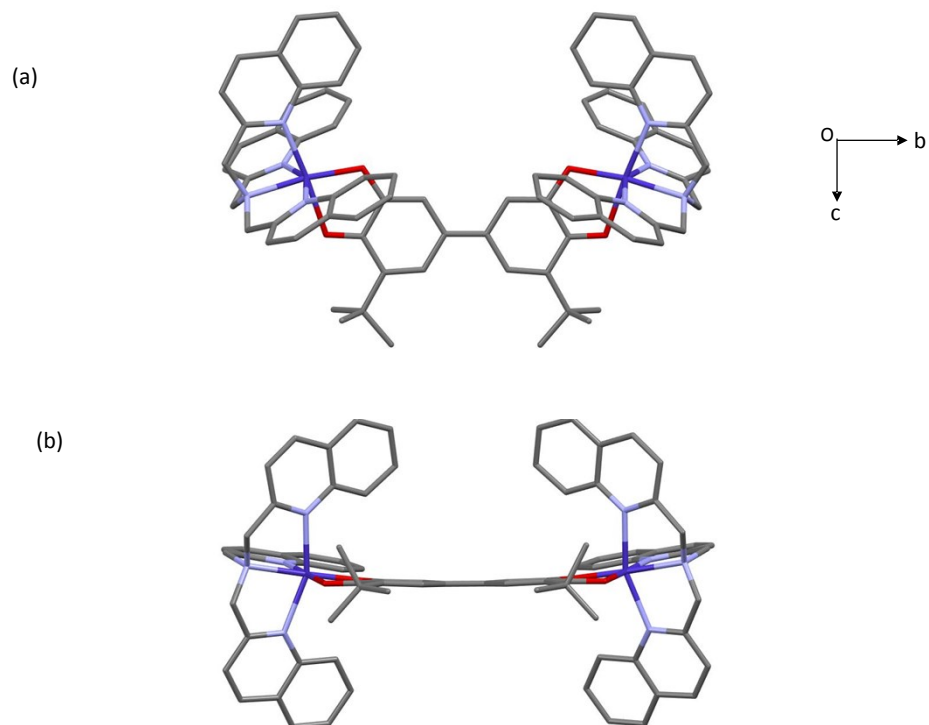


Figure S14. Crystal structure of $[\text{Co}_2(\text{BP})(\text{pbqa})_2](\text{PF}_6)_2$ (**4**). Hydrogen atoms and the PF_6 anions are omitted for the sake of clarity. (a) top view (b) side view.

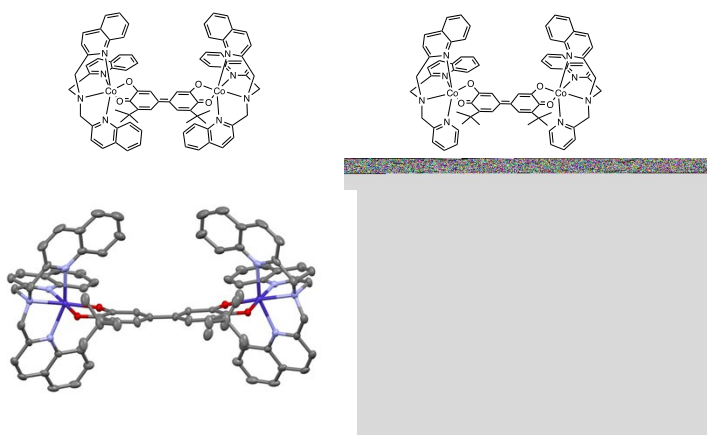


Figure S15. Compared of $[\text{Co}_2(\text{BP})(\text{tqa})_2](\text{PF}_6)_2$ (**5**) (left) and $[\text{Co}_2(\text{BP})(\text{pbqa})_2](\text{PF}_6)_2$ (**4**) (right).

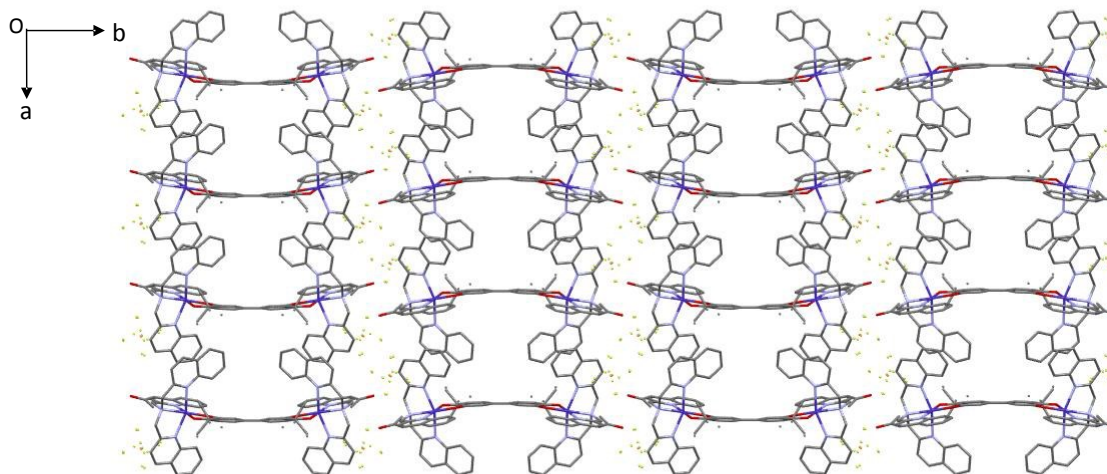


Figure S16. Crystal packing structure of $[\text{Co}_2(\text{BP})(\text{tqa})_2](\text{PF}_6)_2$ (**5**). The upper and lower bent di-nuclear cobalt complexes's structure layers are alternative arranged, and acetone and PF_6^- counter anions are pretend between the layers.

Metrical oxidation state (MOS) calculation

For complex (**4**), dioxolene C-C and C-O bond lengths are correlated to the ligand oxidation state, such that a least-squares fit enables assignment of an apparent metrical oxidation state (MOS, Brown). Catecholite ligands have a MOS of around -0.947 and are characterized as having shorter C-O bonds and longer C-C bonds. Complex (**4**) is assigned $\text{Co}^{\text{II}}\text{-}[\text{Sq-Sq}]\text{-Co}^{\text{II}}$ in the solid state. To determine the Co oxidation state, we used the Co-O, Co-N_{amine}, and Co-N_{qn} bond lengths and octahedral distortion parameter. The calculated Σ

index ($98.3, \Sigma = \sum_{i=1}^{12} |90 - \alpha_i|$ where α_i are the 12 *cis*-O/N-Co-O/N angles about the cobalt atom.) represents the distortion of a coordination environment from an ideal polyhedron. Co(II) has long metal-ligand bonds and distorted octahedral geometries compared to Co(III).

Table S5. MOS values for complex (**4**)

Instructions for using the Metrical Oxidation State Calculator:															
Enter the measured bond distances in the appropriate columns C-G according to the numbering scheme at left. The two C-O distances are averaged in cell C, the C2-C3 and C3-C6 distances are averaged in cell E, and the C3-C4 and C5-C6 distances are averaged in cell F. Then enter a guess for the oxidation state of the ligand into column I. Copy the formulas from line 12, columns J-Q, and use Solver to minimize the value in column O by varying the value in column I. The metrical oxidation state will be in column I, and its <i>esd</i> in column Q.															
Compound	Metal	C-O average	C1-C2	C2-C3 avg	C3-C4 avg	C4-C5	Calc. MOS	Calc C-O	Calc C1-C2	Calc C2-C3	Calc C3-C4	Calc C4-C5	sum of sqp	rmsd	esd
BEF91UF	CoII	1.278	1.467	1.413	1.3795	1.436	-0.9465749	1.2820923	1.46272641	1.42736454	1.36742924	1.43188427	0.00040401	0.00868899	0.08586416
pbqa	C1-O	1.3													
	C2-O	1.256													
	C2-C3	1.38													
	C3-C4	1.4													
	C6-C5	1.436													
	C5-C6	1.359													
	C1-C2	1.467													
	C1-C6	1.446													

Table S6. MOS values for complex (5)

Instructions for using the Metrical Oxidation State Calculator:

Enter the measured bond distances in the appropriate columns C-G according to the numbering scheme at left. The two C-O distances are averaged in cell C, the C2-C3 and C3-C5 distances are averaged in cell E, and the C3-C4 and C5-C6 distances are averaged in cell F. Then enter a guess for the oxidation state of the ligand into column I. Copy the formulas from line 12, columns J-Q, and use Solver to minimize the value in column D by varying the value in column I. The metrical oxidation state will be in column I, and its *end* in column Q.

Compound	Metal	C-O average	C1-C2	C2-C3 avg	C3-C4 avg	C4-C5	Calc. MOS	Calc. C-O	Calc. C3-C2	Calc. C2-C3	Calc. C3-C4	Calc. C4-C5	sum of sqs	rmsd	end
BEFXUF	CoII	1.369	1.491	1.433	1.3855	1.437	-0.7799543	1.37052883	1.47493213	1.4331796	1.36362195	1.43963213	0.00115331	0.01518754	0.14100985
sq	C1-O	1.393													
	C2-O	1.345													
	C2-C3	1.372													
	C3-C4	1.42													
	C4-C5	1.437													
	C5-C6	1.351													
	C1-C2	1.491													
	C1-C6	1.454													

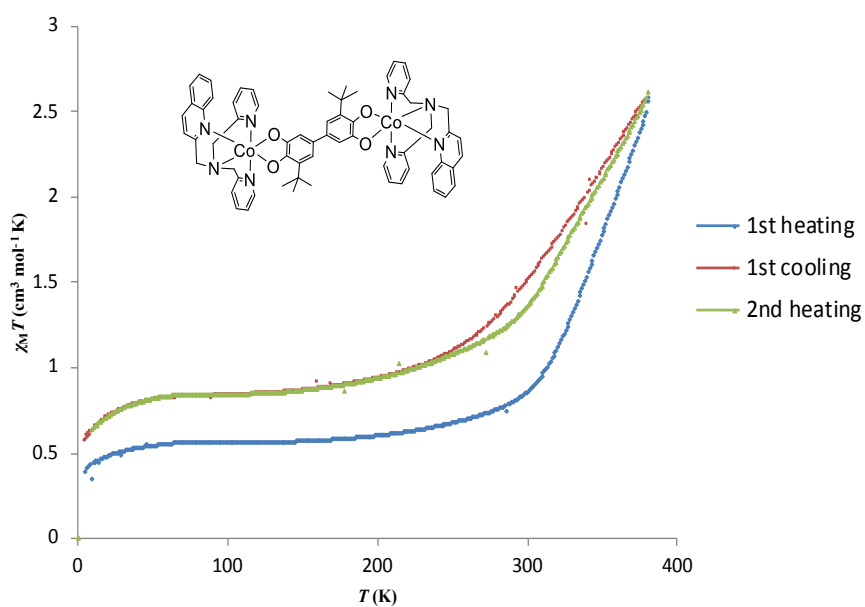


Figure S17. Magnetic susceptibility of $[\text{Co}_2(\text{BP})(\text{bpqa})_2](\text{PF}_6)_2$ (**3**). Repeated data for heating and cooling for samples.